# DIRECT PHOTONS FROM $\psi(3100)$ DECAY*

Michael T. Ronan

Lawrence Berkeley Laboratory
Berkeley, California 94720

## SUMMARY

I will present new results from the Lead Glass Wall experiment (SP26) at SPEAR. We have been motivated by recent Quantum Chromodynamics (QCD) calculations,[1,2] for the $\gamma + 2$ gluons decay mode of orthocharmonium, to search for direct photons from $\psi(3100)$ decay. We have measured inclusive $\gamma$ and $\pi^0$ production from $\psi(3100)$ decay using the Lead Glass Wall addition to the Mark I detector. We compare $\pi^0$ and charged $\pi$ production and calculate the $\pi^0$ decay contribution to the inclusive $\gamma$ spectrum. We find an excess of $\gamma$'s which is partly explained by $\eta$ production and decay, but a signal of high energy direct photons remains. We compare this excess of direct photons with QCD predictions and previously measured 'radiative' decays of the $\psi(3100)$.

## INTRODUCTION

Hadronic decays of the $\psi(3100)$ are described in quantum chromodynamics (QCD) as resulting primarily from the annihilation of a charmed quark and an anti-charmed quark ($c\bar{c}$) into three gluons. The gluons then fragment into hadrons with unit probability in an unknown way (Fig. 1a). The $\psi(3100)$ can also decay into hadrons electromagnetically by the QED coupling of the $c\bar{c}$ pair to a virtual photon which then produces a quark-antiquark pair with each quark fragmenting into hadrons, as in $e^+e^- \to$ hadrons at the same energy, (Fig. 1b). QCD also predicts annihilation into a $\gamma$ and two gluons, with gluon fragmentation into hadrons, to occur at a significant rate: 12% of the three gluon rate[1,2] (for a strong coupling constant value $\alpha_s = 0.2$), (Fig. 1c). The expected $\alpha/\alpha_s$ suppression for the $\gamma$-2 gluon decay relative to the 3-gluon decay is enhanced by a Bose statistical factor of 3!/2!, for there are only two identical particles in the former and three in in the latter decay.

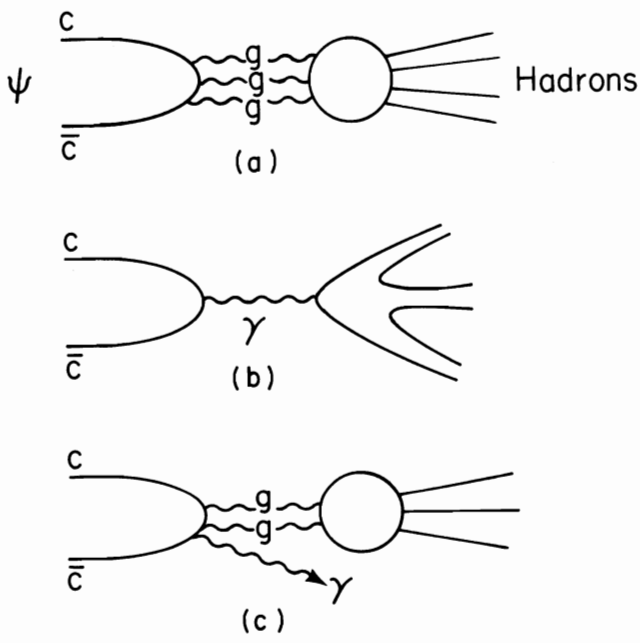


Fig. 1. Schematic diagram for $\psi(3100)$ decays into hadrons through (a) three gluons and (b) a single photon; (c) shows the decay into a $\gamma$ plus hadrons through a $\gamma$-2 gluon intermediate state. In QCD, the decay of a color singlet $1^{--}$ state into one gluon is forbidden by color conservation, while the decays into two photons, two gluons or one photon and a gluon are forbidden by C-parity. XBL 799-2973

We convert the $\gamma$-2 gluon to 3 gluon ratio of partial widths, $\Gamma(\gamma\text{-2 gluons})/\Gamma(3\text{ gluon}) = 0.0234/\alpha_s$,[1,2] to the ratio of the $\gamma$-2 gluon decay to all hadronic decays of the $\psi$ assuming that the processes listed above account for the full $\psi$ partial width into hadrons, $\Gamma(\text{hadrons}) = 57 \pm 11$ keV;[3] that is,

$$\Gamma(\text{hadrons}) = \Gamma(3\text{ gluons}) + \Gamma(\gamma^* \to \text{hadrons}) + \Gamma(\gamma\ 2\text{ gluons}).$$

Using $\Gamma(\gamma^* \to \text{hadrons}) = 12 \pm 2$ keV,[4] we obtain

$$\Gamma(\gamma\ 2\text{ gluons})/\Gamma(\text{hadrons}) = (0.0185 \pm 0.0013)/(\alpha_s + 0.0234),$$

which equals $(8.3 \pm 0.6)\%$ for $\alpha_s = 0.2$. The $\gamma$ momentum spectrum in this process is expected to increase linearly with momentum[2] in contrast to the approximately exponential decrease of $\gamma$'s from $\pi^0$ decay.

The possibility of observing this high momentum QCD $\gamma$ signal has motivated us to investigate the $\gamma$ spectrum in $\psi(3100)$ decay. As pointed out by Ellis in these proceedings, higher order QCD corrections have not been worked out in many QCD decays (for example, in $\psi \to \gamma + 2$ gluons) and in some cases where the calculations have been carried out (for example, the decay of paracharmonium into $2\gamma$'s) the next order term is as large as the lowest order term. In addition, the $\gamma$ momentum spectrum will be affected by resonances in the recoil system. Thus we use QCD only as a guide. We note that 'radiative' decays of the $\psi$ (i.e., $\psi \to \pi^0\gamma$, $\eta\gamma$, ...) are expected to contribute to the $\gamma$ momentum spectrum at high momentum and cannot be separated from the $\gamma + 2$ gluons decay contribution. Indeed these decays (except for $\psi \to \pi^0\gamma$) may proceed through a $\gamma + 2$ gluons intermediate state.

The experiment was run at SPEAR with the Stanford Linear Accelerator Center–Lawrence Berkeley Laboratory magnetic detector,[5] augmented by the Lead-Glass Wall[6] for e and $\gamma$ detection (Fig. 2). The Lead-Glass Wall consists of two layers of lead glass counters (an inner $2 \times 26$ active converter array of $10.8 \times 90$ cm$^2$ counters 3.3 radiation lengths thick and an outer $14 \times 19$ array of $15 \times 15$ cm$^2$ counters 10.5 radiation lengths thick) and three planes of magnetostrictive spark chambers (two placed outside the one-radiation-length thick aluminum magnet coil of the central detector and one between the two layers of lead glass) (Fig. 3). The fiducial region of the wall used in this analysis covers approximately $0.049 \times 4\pi$ sr.

*This work was supported by the High Energy Physics Division, Office of Basic Energy Science of the U.S. Department of Energy under contract W-7405-ENG-48.

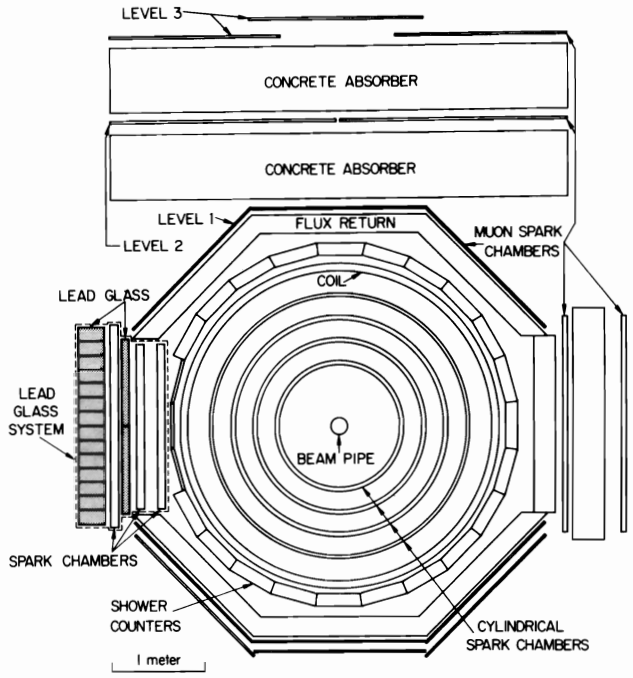


XBL 7711-10393

Fig. 2. The SPEAR magnetic detector[5] as seen looking along the beam line. The proportional chambers around the beam pipe and the trigger counters are not shown. The Lead Glass Wall (LGW)[6] is shown on the left.

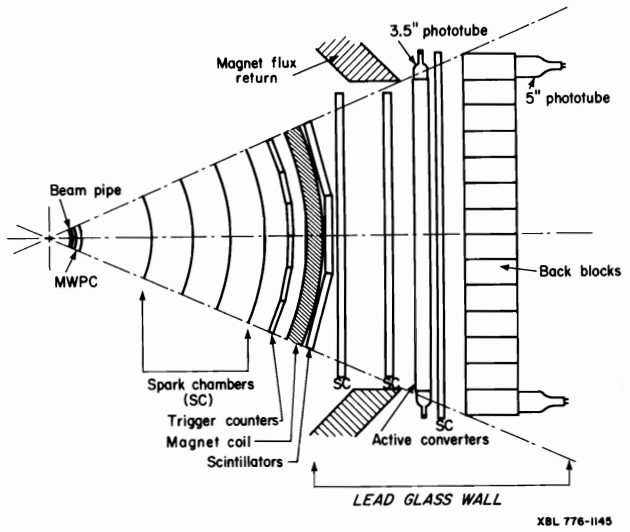


XBL 776-1145

Fig. 3. Expanded view of the Lead Glass Wall octant of the magnetic detector.

## INCLUSIVE γ PRODUCTION

We identify γ's as energy deposits in the lead glass counters, which are not associated with charged particle tracks projected from the central detector. Correlating the spark chamber information with the lead glass energy distribution improves the spatial localization of the γ's to approximately 2 cm. The resulting angular resolution is $\Delta\theta \cong 0.5°$. Conversion of γ's in the aluminum magnet coil is tagged by tracks in the two spark chambers between the coil and the active converter array and a correction is made for an average energy loss in the coil of about 50 MeV. The γ energy resolution was measured using the reaction $e^+e^- \to \gamma\gamma$ to be $\Delta E/E \cong 0.08/\sqrt{E}$ at E = 1.89 GeV and its energy dependence was taken to follow $\Delta E/E \propto 1/\sqrt{E}$ as measured for electrons from $e^+e^- \to e^+e^-$.

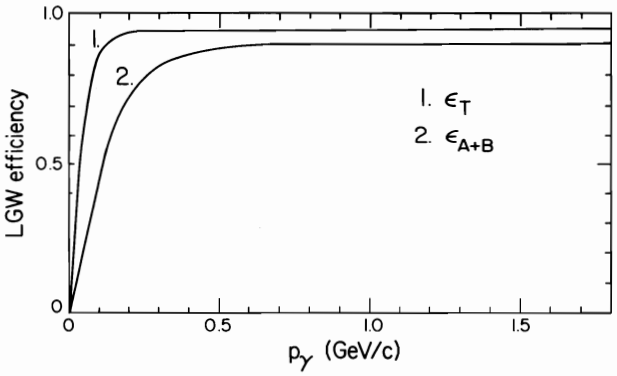


Fig. 4. Efficiency for detecting γ's in the LGW. The curve labeled 1 is the overall efficiency. While the curve labeled 2 is for the category of γ's used in this analysis; that is, γ's which deposit energy in the active converter, layer A, and the outer B layer and, as a result of requiring energy deposition in both layers, have the least background. XBL795-1676

In the Lead Glass Wall (LGW) measurement we use only γ's which deposit energy in both the active converter and outer array to reduce backgrounds. The identification efficiency and the geometrical acceptance of the LGW was calculated using the Monte Carlo shower development program EGS.[7] This identification efficiency times acceptance is shown in Fig. 4 as the curve labeled $\varepsilon_{AB}$. The calculation includes the loss of γ's due to conversion in the beam pipe material since these γ's do not appear in the LGW sample. We assign a systematic error of 5% to this correction except for $p_\gamma < 300$ MeV/c where we use a 30% error.

The data sample used in this analysis consists of about 80,000 $e^+e^- \to \psi(3100) \to$ hadron events with at least two detected charged particles in the central detector. If only two oppositely charged particles are detected, they are required to be acoplanar with the beams by at least 20°. Two classes of events in this sample are considered in the analysis: those with at least one γ which has converted in the material (0.05 radiation lengths) surrounding the beam intersection region, and those with at least one photon detected in the Lead Glass Wall.

To determine the γ inclusive spectrum, one needs a trigger efficiency and charged particle acceptance correction which compensates for the loss of neutral events and events with less than two detected charged particles. The γ conversion events are used to measure this trigger efficiency times acceptance since the $e^+e^-$ conversion pair triggers the detector and satisfies the two or more charged particle requirement in the event selection. This gives us a sample of events with a γ and anything else, including all neutrals. The trigger efficiency times acceptance shown in Fig. 5 is just the fraction of this sample which would have triggered if the γ had not converted near the beam pipe and is used in the analysis of the γ's in the Lead Glass Wall. It is independent of $x_\gamma = p_\gamma/E_{beam}$ within our statistics and has an average value of 37%. We use this average value for $x_\gamma < 0.15$.

The γ inclusive spectrum for γ's in the Lead Glass Wall corrected for a constant trigger efficiency times charged particle acceptance and the γ identification times acceptance of the LGW is shown in Fig. 6. The

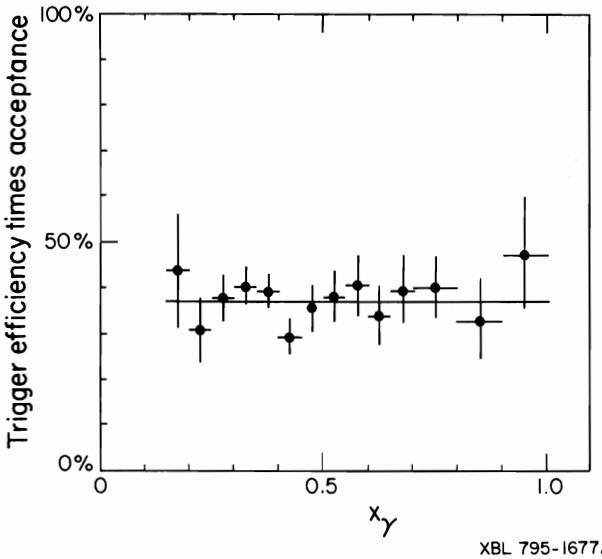


XBL 795-1677A

Fig. 5. Trigger efficiency times acceptance for two or more particles for events in the magnetic detector with a $\gamma$ with $|\cos\theta| \leq 0.476$ vs. $x_\gamma$ $(=p_\gamma/E_{beam})$. Measured using photons which convert near the beam pipe and produce a $e^+e^-$ pair which satisfies the trigger requirement.

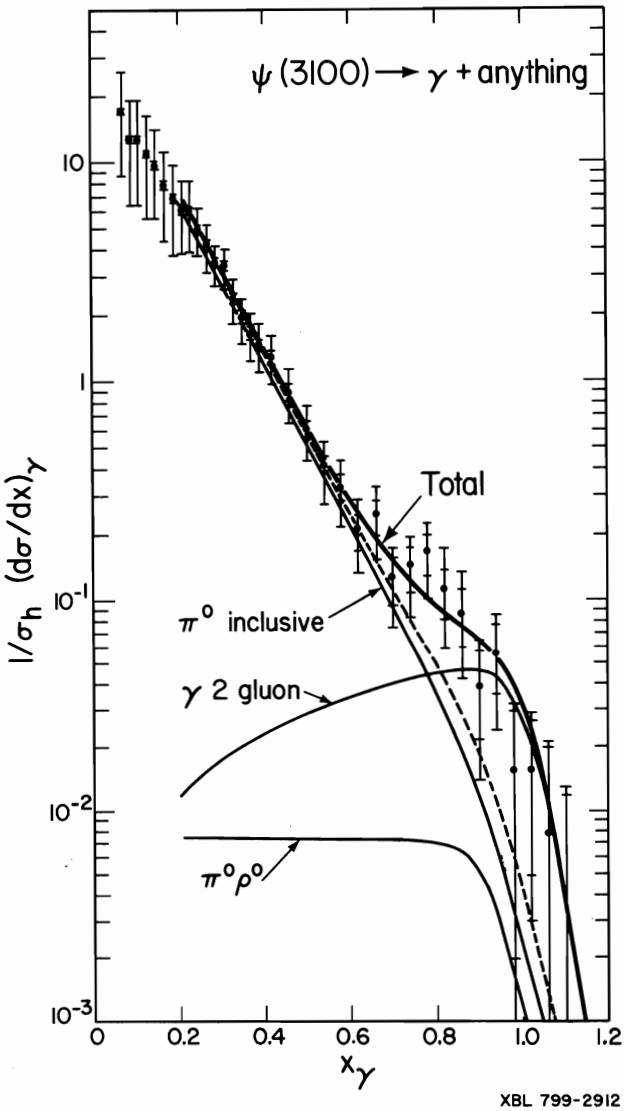


XBL 799-2912

Fig. 6. Inclusive $\gamma$ spectrum from $\psi(3100)$ decay, normalized to all hadronic decays of the $\psi$. The "$\pi^0$ inclusive" and "$\pi^0\rho^0$" curves show the expected contributions to the $\gamma$ spectrum from $\pi^0$'s. The dashed curve shows the sum of the "$\pi^0$ inclusive" curve renormalized upward by 1.12 and the "$\pi^0\rho^0$" curve. The curve labeled "$\gamma$ 2 gluon" is the $\gamma$ spectrum expected from $\psi \rightarrow \gamma + 2$ gluons $\rightarrow \gamma$ + hadrons.[2] The result of a fit to the data with the $\pi^0$ decay contributions and the "$\gamma$ 2 gluon" spectrum is shown as the curve labeled "Total".

inner error bars shown are statistical while the outer error bars include the systematic error added in quadrature. These systematic errors are obtained mainly from the statistical errors in the trigger efficiency of Fig. 5. The curves in Fig. 6 are described below.

## INCLUSIVE $\pi^0$ PRODUCTION

We measure $\pi^0$ production in events with two or more charged particles in the central detector and two or more photons detected in the Lead Glass Wall. We require the $\gamma$ energy to be at least 100 MeV and the energy of each $\gamma\gamma$ pair to be at least 0.25 times the beam energy (i.e., $x_{\gamma\gamma} = 2E_{\gamma\gamma}/m_\psi > 0.25$). The $\gamma\gamma$ invariant mass spectrum is shown in Fig. 7. We observe a clean $\pi^0$ signal with a resolution of about 17 MeV/$c^2$. The background under this signal has been obtained by pairing uncorrelated $\gamma$'s from separate events, requiring the minimum separation in angle

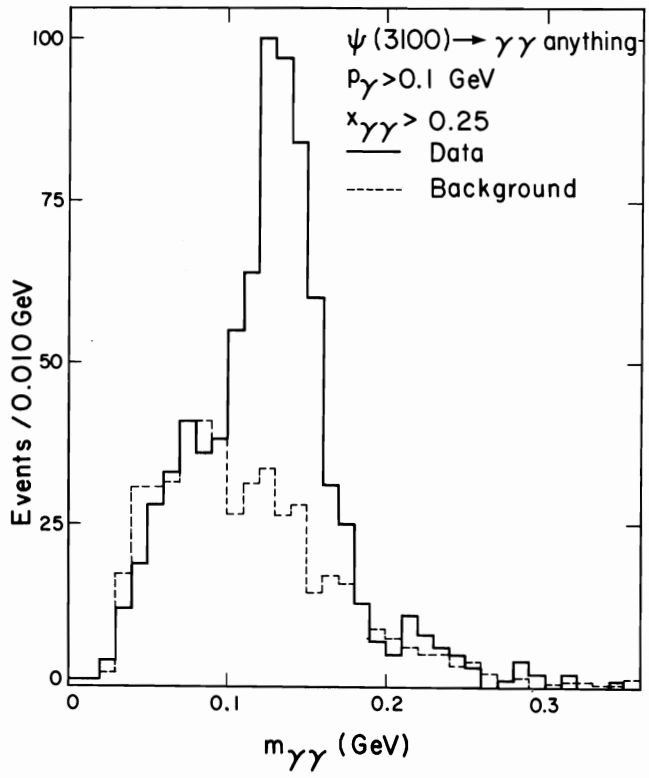


Fig. 7. The $\gamma\gamma$ invariant mass for events with $x_{\gamma\gamma}$ $(=2p_{\gamma\gamma}/m_\psi) > 0.25$. The background under the $\pi^0$ peak has been calculated by combining single $\gamma$'s from two different events and has been normalized to the measured points outside the peak.

necessary to separate the $\gamma$'s if they appeared in the same event and after normalizing the background to the data outside the $\pi^0$ peak in each of several $x_{\gamma\gamma}$ bins. The estimated background is in reasonably good agreement in shape with the data outside the $\pi^0$ peak and gives a signal of 267 $\pi^0$'s with $110 \leq m_{\gamma\gamma} < 160$ MeV/c . We have compared the measured shape of the $\pi^0$ signal with a Monte Carlo calculation based on EGS to correct for the fraction of $\pi^0$'s outside our cut. We correct for 22% of the $\pi^0$'s which are reconstructed outside of the selected $m_{\gamma\gamma}$ range and assign a 10% systematic error to the corrected number of $\pi^0$'s to account for our uncertainty in the background estimation and the mass resolution.

We have used EGS and a model of the Lead Glass Wall to determine the $\pi^0$ identification efficiency and geometrical acceptance shown in Fig. 8. The loss of efficiency above 1.5 GeV is due to overlap of the $\gamma$

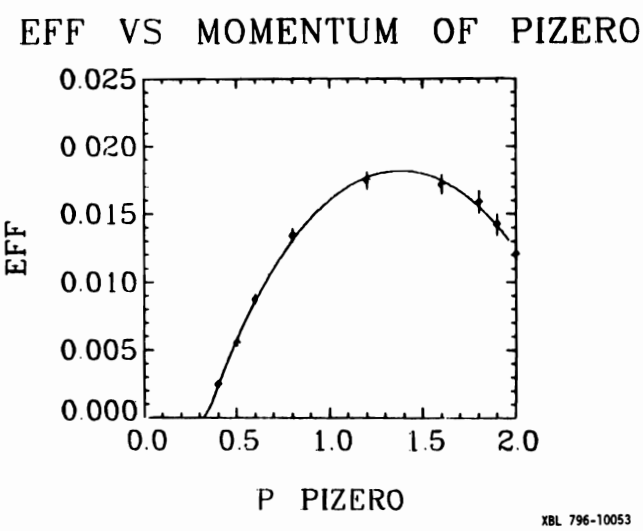


Fig. 8. Lead Glass Wall identification efficiency times acceptance for $\pi^0$'s versus $\pi^0$ momentum in GeV/c.

showers in the lead glass counters. We calculate the $\pi^0 \to 1'\gamma'$ misidentification probability is less than a few percent for the maximum $\pi^0$ energy from $\psi(3100)$ decay. We have used a model of the Mark I detector and a statistical model for $\psi(3100)$ decay to determine a trigger efficiency times two charged particle acceptance of $(0.33 - 0.11\ x^2_{\pi^0})$. We estimate systematic errors of 10% in our calculation of the $\pi^0$ identification efficiency of the LGW and 10% for the trigger efficiency times acceptance correction. The $x_{\pi^0} = 2p_{\pi^0}/m_\psi$ distribution of the corrected data is shown in Fig. 9, where the inner error bars are the statistical errors and the outer error bars are the statistical and 17% systematic errors added in quadrature.

We compare our measured $\pi^0$ spectrum to $\pi^\pm$ production since for an $I_{spin} = 0$ state like the $\psi(3100)$ we expect $\pi^0$ production to be one-half of charged production for the dominant hadronic decays, as in Fig. 1a. We measure inclusive $\pi^\pm$ production using the same data sample. The measurement is based on the spark chamber system of the magnetic detector which has a resolution of $\Delta p/p \approx 0.013p$ (in GeV/c) over a solid angle of $0.60 \times 4\pi$ sr. A time-of-flight system with resolution of 0.35 nsec is used to obtain a statistical $\pi$-K separation up to 1.0 GeV/c ($x_\pi = 0.65$). We correct for trigger efficiency and acceptance with the same statistical model of $\psi(3100)$ decay used in the $\pi^0$ analysis. The measured $x_{\pi^\pm}$ distribution for $\pi^+$

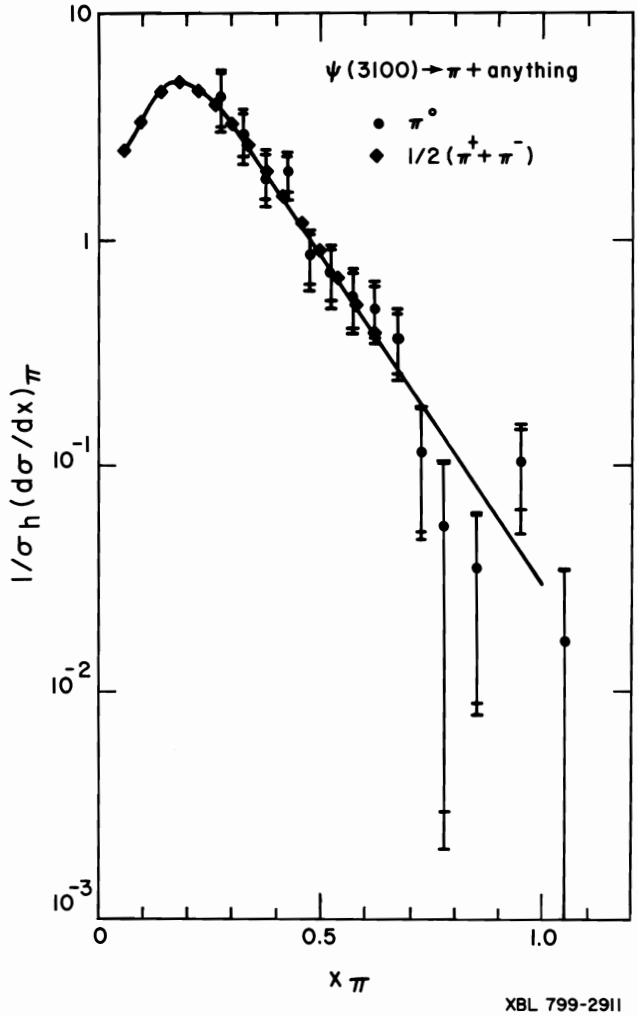


Fig. 9. Inclusive $\pi$ spectra from $\psi(3100)$ decay. The circular points show the $\pi^0$ spectrum and the diamond shaped points show one-half of the charged $\pi$ spectrum. The curve is obtained in a fit described in the text. The high point at $\langle x_{\pi^0} \rangle = 0.95$ is partly due to the $\pi^0\rho^0$ decay of the $\psi(3100)$.

or $\pi^-$ production with $x_{\pi^\pm} < 0.65$ is shown in Fig. 9. Statistical and systematic errors of about 20% are not shown. We find that the $\pi^0$ and charged $\pi$ spectra agree in shape and that the ratio of $\pi^0$ to charged $\pi$ production is $N_{\pi^0}/(N_{\pi^+} + N_{\pi^-}) = 0.52 \pm 0.05$ (stat) $\pm 0.07$ (sys) for $0.25 \leq x_\pi < 0.65$.

The solid curve in Fig. 9 is a hand fit to the measured charged pion data for $x_{\pi^\pm} < 0.40$ which is extrapolated to $x_{\pi^\pm} = 1$ using an exponential fit to the six measured $\pi^\pm$ data points in the $0.40 \leq x_{\pi^\pm} < 0.65$ region. We expect to find an excess of events above this extrapolation in the $\langle x_{\pi^0} \rangle = 0.95$ bin due to the $\pi^0\rho^0$ decay of the $\psi(3100)$, since the charged $\pi$ spectrum has been measured[8] to be exponential to $x_{\pi^\pm} \cong 0.90$ and to exhibit a peak due to $\pi^\pm\rho^\pm$ decay at $x_{\pi^\pm} \cong 0.94$. We find that the $\langle x_{\pi^0} \rangle = 0.95$ point in our $\pi^0$ data is higher than the exponential extrapolation and is consistent with the expected $\pi^0\rho^0$ effect.

## COMPARISON OF $\gamma$ SPECTRUM TO $\pi^0$ DECAY CONTRIBUTION

We now compare the observed spectrum of Fig. 6 with that expected from $\pi^0$ decay. Our estimation of the contribution to the $\gamma$ spectrum from the $\pi^0$ continuum is obtained by Monte Carlo generation and decay of

$\pi^0$'s according to the spectrum shown as a solid curve in Fig. 9 with the absolute normalization determined from our $\pi^0$ measurement. The resulting $\gamma$ spectrum is shown in Fig. 6 with the label "$\pi^0$ inclusive". The $\pi^0\rho^0$ contribution is shown separately with its normalization determined by the measured $\psi \to \pi\rho$ branching fraction $(1.1 \pm 0.2)\%$ [3] and a $(1+\cos^2\theta_{\pi^0})$ angular distribution. The shape is a flat spectrum up to $x_\gamma = 0.934$ smeared by an $8\%/\sqrt{E}$ resolution. We subtract the "$\pi^0$ inclusive" and "$\pi^0\rho^0$" curves of Fig. 6 from the data to obtain the subtracted spectrum of Fig. 10. The inner error bars are the statistical errors from the $\gamma$ spectrum, while the outer error bars are the statistical and systematic errors added in quadrature. These systematic errors include our uncertainty in the $\pi^0$ decay contribution obtained using the solid curve of Fig. 9.

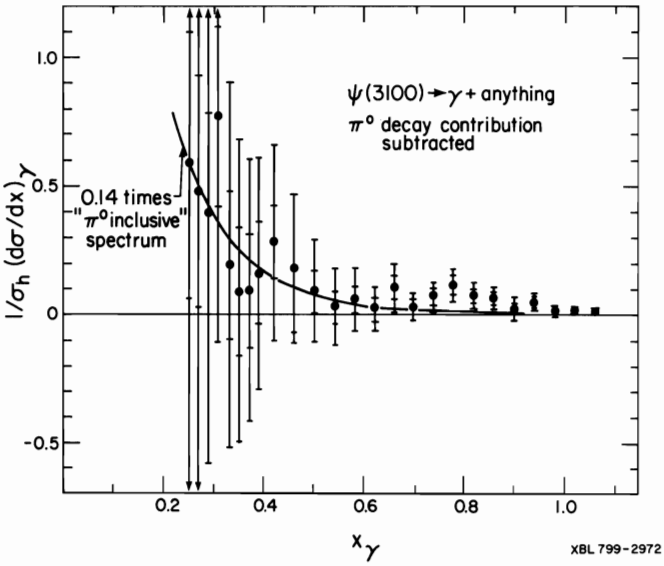


Fig. 10. Subtracted $\gamma$ spectrum. We show the $\gamma$ spectrum with the absolutely normalized $\pi^0$ decay contribution subtracted. The solid curve is the "$\pi^0$ inclusive" decay contribution (from Fig. 6) times 0.14.

We observe that the subtracted spectrum of Fig. 10 shows an excess of $\gamma$'s above that expected from $\pi^0$ decay. At low $x_\gamma$ the measured excess is within our systematic errors while the excess for $x_\gamma > 0.6$ is above systematic errors and has a magnitude of $(2.8 \pm 0.5^{+1.6}_{-0.9})\%$ of all hadronic $\psi$ decays assuming a $(1+\cos^2\theta_\gamma)$ angular distribution. The systematic error here includes: our uncertainties in the spectrum (±11%, which is mainly the 10% statistical error in the measurement of the trigger efficiency of Fig. 5 for $x_\gamma > 0.6$), and a 20% error in the $\pi^0$ decay contribution. We add an additional +20% asymmetric error to account for a 20% increase in the measured excess if we use the measured $\pi^0$ points for $x_{\pi^0} > 0.6$ to calculate the expected $\pi^0$ decay contribution instead of the fit to the charged particle data (solid curve of Fig. 9).

$\eta$ production and decays into $\gamma$'s will contribute to the measured excess. $\psi \to \eta$ + anything has not been previously measured and the Lead Glass Wall has very low acceptance for $\eta \to \gamma\gamma$. However, Monte Carlo studies show that if the $\eta$ inclusive spectrum is similar to the $\pi^0$ spectrum,[9] then the resulting $\gamma$ spectrum would be similar to the "$\pi^0$ inclusive" spectrum of Fig. 6 for $x_\gamma \geq 0.2$. We show in Fig. 10 the "$\pi^0$ inclusive" contribution of Fig. 6 scaled by a factor of 0.14. We observe that the low energy excess is consistent with an $\eta$ contribution similar to the $\pi^0$ contribution (or, with a systematic error in our relative $\gamma$ and $\pi^0$ normalization). We note that an $\eta/\pi^0$ ratio of 4 to 5 at $x \cong 1$ would be required to explain the high energy $\gamma$ excess. Thus we find an apparent excess of high energy $\gamma$'s above the expected sources of indirect $\gamma$'s.

We have considered a number of possible sources of the apparent excess $\gamma$'s, such as: (1) $\pi^0$ misidentification as a single cluster in the Lead Glass Wall, (2) a non-Gaussian resolution function for the energy measurement, and (3) unknown systematic errors in the analysis of the LGW data. We have calculated that effect (1) is negligible in the $\psi(3100)$ data sample. (We note that the lead glass counters are 15 $cm^2$, while the minimum separation for $2\gamma$'s from $\pi^0$ decay is about 40 cm for the maximum energy $\pi^0$ from $\psi$ decay. Also, the measure transverse energy spread of the $\gamma$ clusters with $x > 0.8$ are all less than 10 cm.) Figure 11 shows the $\gamma$ energy distribution for $\gamma$'s from $e^+e^- \to \gamma\gamma$ at

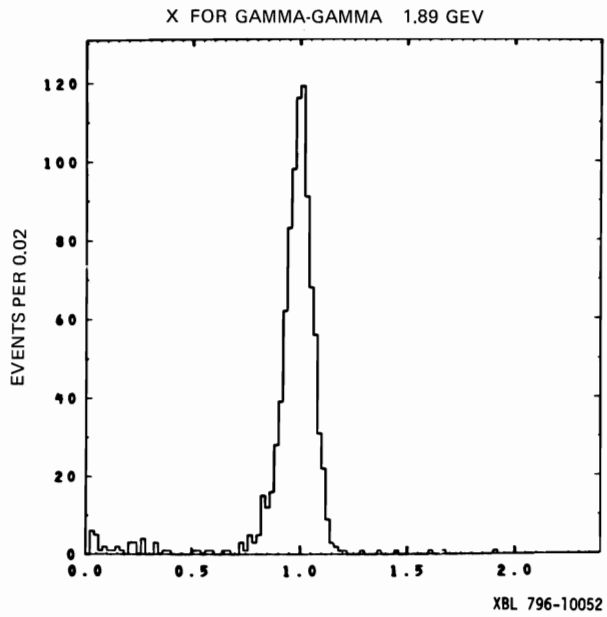


Fig. 11. Ratio of the measured $\gamma$ energy to the beam energy for $\gamma$'s from $e^+e^- \to \gamma\gamma$. The data were taken at the $\psi(3772)$ with a neutral energy trigger.

1.89 GeV. We note that there is no significant high energy tail to the measured distribution over about 2 orders of magnitude. We have a check of the LGW data and effect (3) by measuring the $\gamma$ distribution using the $\gamma$'s which have converted in the material surrounding the beam pipe. This $\gamma$ sample has been corrected for the conversion probability, the tracking efficiency for the $e^+e^-$ pair and for cuts used to separate these events. The resulting $\gamma$ spectrum is shown in Fig. 12, where the outer error bars include a 20% systematic error added in quadrature to the statistical errors. An additional 20% momentum-indpendent systematic error has not been shown. We also show the expected $\pi^0$ decay contribution (the measured $\pi^0$ inclusive contribution plus the $\pi^0\rho^0$ contribution). Although the errors are large, we note that these data follow a shallower slope than the expected $\pi^0$ decay contribution (all the points for $x_\gamma > 0.6$ are systematically above the curve), and the measured excess for these data, $(2.1 \pm 1.2 \pm 1.7)\%$ of all hadronic $\psi$ decays, is in good agreement with the LGW result. We have no check of the $\pi^0$ spectrum,

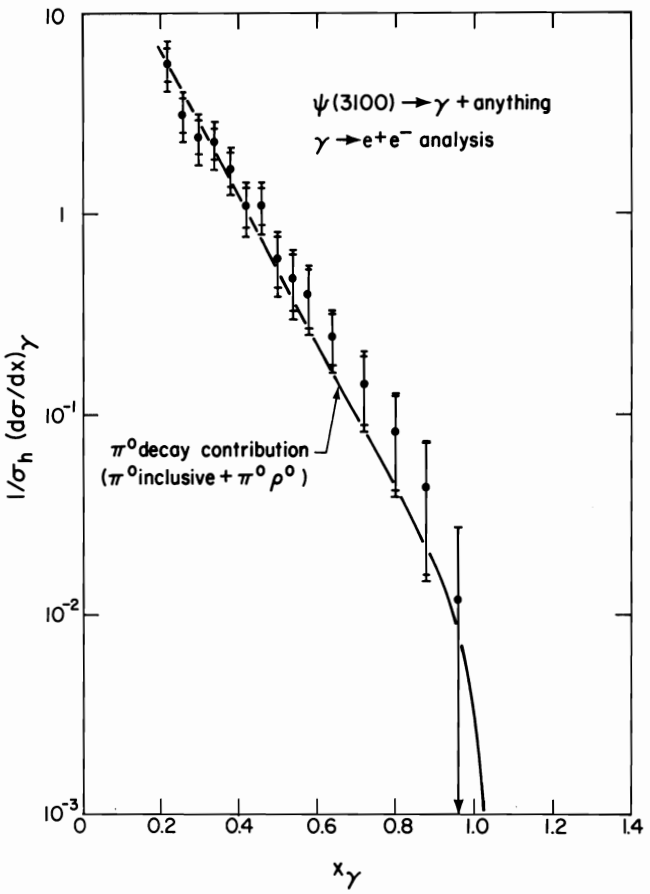


Fig. 12. Inclusive γ spectrum from ψ(3100) decay measured using converted photons. The curve is the calculated $\pi^0$ decay contribution. (XBL799-2971)

however, we note that the $\pi^0$ and charged π spectra for this experiment and Reference 8 agree in shape to $x \cong 1$, and that the γ inclusive data shows an excess of high energy photons over a simple exponential extrapolation of the low energy γ spectrum.

Possible backgrounds to the measured direct photon excess are: indirect source of γ's, fake γ events and γ's not from ψ(3100) decay but due to beam-related or QED backgrounds. We find no other likely indirect source of high energy γ's besides the $\pi^0$ and η, since other mesons give a soft γ contribution. Fake γ events could be due to $\bar{n}$ annihilation in the Lead Glass Wall. We used an inclusive measurement of $\bar{p}$ production from our data to estimate this background to be less than a 10% effect. Photons from beam related or QED backgrounds might show up in the $\cos\theta_\gamma$ distribution as a peaking at small angles (i.e., close to the beam axis). The observed $\cos\theta_\gamma$ distribution for high energy γ's does not show this effect. Also, the measured excess of hadronic events with a high energy photon corresponds to a cross section of about 2.5 units of R ($=\sigma/\sigma_{\mu\mu}$), and thus the effect is from ψ(3100) decay.

## COMPARISON OF EXCESS γ's TO QCD PREDICTIONS

To compare the measured excess of high momentum γ's with QCD predictions for the γ + 2 gluons decay mode of the ψ(3100), we perform a maximum likelihood fit to the data with the sum of the "$\pi^0$ inclusive" and "$\pi^0\rho^0$" spectra and a "γ 2 gluon" spectrum of the form given in Reference 2 folded with an $8\%/\sqrt{E}$ resolution, as shown in Fig. 6. The normalizations of the "$\pi^0$ inclusive" and "γ 2 gluon" spectra are the two free parameters of the fit while the "$\pi^0\rho^0$" spectrum normalization is fixed as discussed above. This procedure allows for an η contribution similar to the $\pi^0$ contribution (and also allows for $x_\gamma$ independent systematic errors in the $\pi^0$ to γ relative normalizations). The sum of the three spectra, labeled "Total" in Fig. 6, fits the data well with a $\chi^2$ per degree-of-freedom of about 1. The "$\pi^0$ inclusive" spectrum renormalization factor obtained is 1.12. The sum of the renormalized "$\pi^0$ inclusive" contribution and the "$\pi^0\rho^0$" contribution is shown as the dashed curve in Fig. 6. We find an excess of γ's with $x_\gamma > 0.6$ remains. The magnitude of this excess is $(2.4 \pm 0.5^{+1.6}_{-0.9})\%$ of all hadronic decays of the ψ(3100) assuming a $(1+\cos^2\theta_\gamma)$ angular distribution as predicted for the γ + 2 gluon decay (see discussion below also).

Using the QCD spectrum to correct for the low energy part of the spectrum which we don't measure, we find that if the excess is due to the γ + 2 gluons decay mode of the ψ(3100), then

$$\Gamma(\psi \to \gamma + 2 \text{ gluons})/\Gamma(\psi \to \text{hadrons}) = (3.5 \pm 0.7^{+2.3}_{-1.2})\%.$$

This is smaller than the 8.3% predicted[3] by QCD for $\alpha_s = 0.2$ and it could be explained by a higher strong coupling constant value in the range $\alpha_s = 0.3 - 0.7$. Figure 13 shows the γ spectrum at high $x_\gamma$ with the renormalized "$\pi^0$ inclusive" and "$\pi^0\rho^0$" contributions (dashed curve of Fig. 6) subtracted. Systematic errors which vary in magnitude from 0.08 to 0.02 from $x_\gamma = 0.6$ to 1.0, are not shown. The solid curve is the "γ 2 gluon" spectrum of Fig. 6. We note that the measurement errors are large enough that we are insensitive to the linearly rising shape of the "γ 2 gluon" spectrum (a flat spectrum, for example, would fit the data as well).

The dashed curve in Fig. 13 is the expected distribution for the sum of the measured[10] processes $\psi \to \gamma\pi^0$, γη, γη', and γf smeared by the $8\%/\sqrt{E}$ resolution. Note that these decays, except for the γf, produce a $(1+\cos^2\theta_\gamma)$ angular distribution. We find that the measured exclusive processes account for

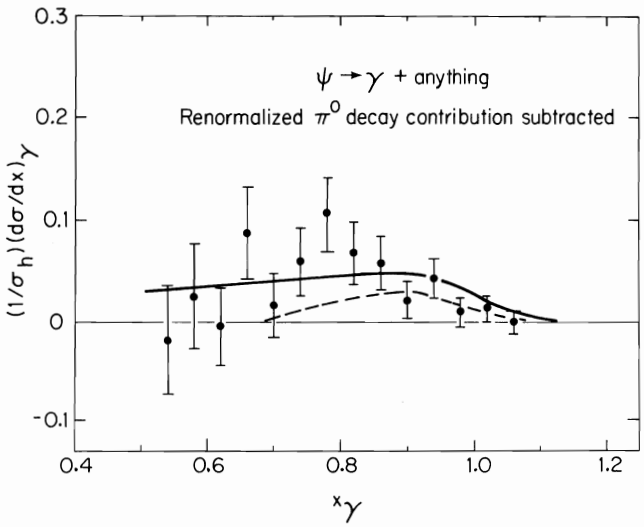


Fig. 13. Subtracted γ spectrum. Here we show the γ spectrum by subtracting the sum of the renormalized $\pi^0$ inclusive and the $\pi^0\rho^0$ decay contributions (dashed curve of Fig. 6). Systematic errors, which are not shown, vary in magnitude from about 0.08 at $x_\gamma = 0.6$ to 0.02 at $x_\gamma \cong 1$. The solid curve is the γ + 2 gluons prediction and the dashed curve is the expected γ distributions from the measured[10] exclusive processes $\psi \to \gamma\pi^0$, γη, γη' and γf.
(XBL 7910-4261)

about 25% of the observed excess for $x_\gamma > 0.6$. However, these final states (except for the $\pi^0\gamma$, which is suppressed in any case[10]) could be produced via a $\gamma + 2$ gluons intermediate state with the 2 gluons coupling to the final state meson. In particular, the large $\psi \to \gamma f/\psi \to \gamma\pi^0$ ratio[11] might be explained as being due to the odd G-parity of the $\pi^0$ and a non-zero f-gluon-gluon coupling.

## CONCLUSION

We have measured inclusive $\gamma$ and $\pi^0$ production in $\psi$ decay. We have compared the $\pi^0$ spectrum with $\pi^\pm$ spectrum measured in the same detector and find the $\pi^0$'s to be consistent with one-half of the charged pions. Comparing the $\gamma$ spectrum with that expected from $\pi^0$ decay we observe an excess of high momentum ($x_\gamma \geq 0.6$) photons of magnitude $(2.8 \pm 0.5^{+1.6}_{-0.9})\%$ of all hadronic $\psi$ decays. We have considered the $\eta$ as a possible source of these excess $\gamma$'s and have found that an excess of $(2.4 \pm 0.5^{+1.6}_{-0.9})\%$ remains after one renormalizes the $\pi^0$ contribution upward to allow for an $\eta$ contribution which follows the $\pi^0$ decay contribution. The measured excess can be explained by the QCD decay of the $\psi(3100)$ into $\gamma + 2$ gluons, and in part by previously measured exclusive decays.


## Acknowledgments

I would like to acknowledge the help of all of my collaborators on the Lead Glass Wall experiment, especially Tom Trippe of LBL who worked with me on this analysis. I also would like to thank S. J. Brodsky, M. S. Chanowitz and R. Cahn for many useful discussions.


## FOOTNOTES AND REFERENCES


1. T.Appelquist, A.DeRújula, H.D.Politzer and S.L. Glashow, Phys. Rev. Lett. 34, 365 (1975), footnote 12 — a factor of 3 error was corrected by: M.S.Chanowitz, Phys. Rev. D12, 918 (1975) and L.B.Okun and M.B.Voloshin, ITEP-95 (1976).
2. S.J.Brodsky, T.A.DeGrand, R.R.Horgan, and D.G.Coyne, Phys. Lett. 73B, 203 (1978).
3. Particle Data Group, Phys. Lett. 75B (April 1978).
4. A.M.Boyarski et al., Phys. Rev. Lett. 34, 1357 (1975).
5. J.-E.Augustin et al., Phys. Rev. Lett. 34, 233 (1975).
6. J.M.Feller et al., IEEE Trans. Nucl. Sci. 25, 304 (1978).
7. R.L.Ford and W.R.Nelson, SLAC-210 (1978).
8. W.Braunschweig et al., Phys. Lett. 63B, 115 (1976).
9. We have tried $\eta$ distributions of the form $e^{-p/p^*}$ and $e^{-E/kT}$ where p and E are the momentum and energy of the $\eta$, and where $p^* \cong 220$ MeV, $kT \cong 210$ MeV were obtained from fits to the $\pi^\pm$ spectrum.
10. The $\psi$ decay branching ratios of the final states used here are:
    $BR(\gamma\pi^0) = (7.3 \pm 4.7) \times 10^{-5}$,
    W.Braunschweig et al., Phys. Lett. 67B, 243 (1977);
    $BR(\gamma\eta) = (1.3 \pm 0.4) \times 10^{-3}$,
    W.Bartel et al., Phys. Lett. 66B, 489 (1977);
    $BR(\gamma\eta') = (2.4 \pm 0.7) \times 10^{-3}$,
    W.Bartel et al., Phys. Lett. 64B, 483 (1976);
    $BR(\gamma f) = (2.0 \pm 0.7) \times 10^{-3}$,
    G.Alexander et al., Phys. Lett. 72B, 493 (1978).
11. G.Alexander et al., ibid.